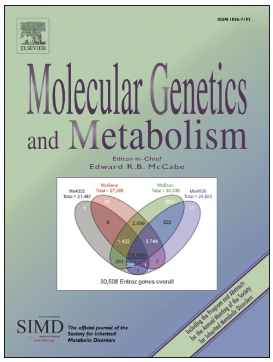

Hypoxia ameliorates brain hyperoxia and NAD+ deficiency in a murine model of Leigh syndrome

Robert M.H. Grange, Rohit Sharma, Hardik Shah, Bryn Reinstadler, Olga Goldberger, Marissa K. Cooper, Akito Nakagawa, Yusuke Miyazaki, Allyson G. Hindle, Annabelle J. Batten, Gregory R. Wojtkiewicz, Grigorij Schleifer, Aranya Bagchi, Eizo Marutani, Rajeev Malhotra, Donald B. Bloch, Fumito Ichinose, Vamsi K. Mootha, Warren M. Zapol

PII: S1096-7192(21)00062-7

DOI: https://doi.org/10.1016/j.ymgme.2021.03.005

Reference: YMGME 6747

To appear in: *Molecular Genetics and Metabolism*

Received date: 1 December 2020

Revised date: 7 March 2021

Accepted date: 7 March 2021

Please cite this article as: R.M.H. Grange, R. Sharma, H. Shah, et al., Hypoxia ameliorates brain hyperoxia and NAD+ deficiency in a murine model of Leigh syndrome, *Molecular Genetics and Metabolism* (2021), https://doi.org/10.1016/j.ymgme.2021.03.005

Hypoxia ameliorates brain hyperoxia and NAD^+ deficiency in a murine model of Leigh syndrome

Robert M. H. Grange[a], Rohit Sharma[b], Hardik Shah[b], Bryn Reinstadler[b], Olga Goldberger[b], Marissa K. Cooper[a], Akito Nakagawa[a], Yusuke Miyazaki[a,c], Allyson G. Hindle[a], Annabelle J. Batten[a], Gregory R. Wojtkiewicz[d], Grigorij Schleifer[a], Aranya Bagchi[a], Eizo Marutani[a], Rajeev Malhotra[e], Donald B. Bloch[a,f], Fumito Ichinose[a], Vamsi K. Mootha[b,**] vamsi@hms.harvard.edu, Warren M. Zapol[a,*] wzapol@mgh.harvard.edu

[a]Anesthesia Center for Critical Care Research, Department of Anesthesia, Critical Care, and Pain Medicine, Harvard Medical School and Massachusetts General Hospital, Boston, Massachusetts, USA

[b]Howard Hughes Medical Institute and Department of Molecular Biology, Massachusetts General Hospital and Harvard Medical School, Boston, Massachusetts, USA

[c]School of Life Sciences, University of Nevada Las Vegas, Las Vegas, Nevada, USA

[d]Center for Systems Biology, Harvard Medical School and Massachusetts General Hospital, Boston, Massachusetts, USA

[e]Cardiology Division and Cardiovascular Research Center, Department of Medicine, Harvard Medical School and Massachusetts General Hospital, Boston, Massachusetts, USA

[f]Division of Rheumatology, Allergy and Immunology, Department of Medicine, Harvard Medical School and Massachusetts General Hospital, Boston, Massachusetts, USA

[*]**Corresponding author at:** Anesthesia Center for Critical Care Research, Department of Anesthesia, Critical Care and Pain Medicine, Massachusetts General Hospital and Harvard Medical School, 55 Fruit Street, Thier 503, Boston, MA 02114, USA

[**]**Corresponding author at:** Howard Hughes Medical Institute and Department of Molecular Biology, Massachusetts General Hospital and Harvard Medical School, 185 Cambridge St Boston MA 02114, USA

Abstract

Leigh syndrome is a severe mitochondrial neurodegenerative disease with no effective treatment. In the *Ndufs4*$^{-/-}$ mouse model of LS, continuously breathing 11% O_2 (hypoxia) prevents neurodegeneration and leads to a dramatic extension (~5-fold) in lifespan. We investigated the effect of hypoxia on the brain metabolism of *Ndufs4*$^{-/-}$ mice by studying blood gas tensions and metabolite levels in simultaneously sampled arterial and cerebral internal jugular venous (IJV) blood. Relatively healthy *Ndufs4*$^{-/-}$ and wildtype (WT) mice breathing air until postnatal age ~38 d were compared to *Ndufs4*$^{-/-}$ and WT mice breathing air until ~38 days old followed by 4-weeks of breathing 11% O_2. Compared to WT control mice, *Ndufs4*$^{-/-}$ mice breathing air have reduced brain O_2 consumption as evidenced by an elevated partial pressure of O_2 in IJV blood ($P_{ijv}O_2$) despite a normal PO_2 in arterial blood, and higher lactate/pyruvate (L/P) ratios in IJV plasma revealed by metabolic profiling. In *Ndufs4*$^{-/-}$ mice, hypoxia treatment normalized the $P_{ijv}O_2$ and L/P ratios, and decreased levels of nicotinate in IJV plasma. Brain concentrations of nicotinamide adenine dinucleotide (NAD^+) were lower in *Ndufs4*$^{-/-}$ mice breathing air than in WT mice, but preserved at WT levels with hypoxia treatment. Although mild hypoxia (17% O_2) has been shown to be an ineffective therapy for *Ndufs4*$^{-/-}$ mice, we find that when combined with nicotinic acid supplementation it provides a modest improvement in neurodegeneration and lifespan. Therapies targeting both brain hyperoxia and NAD^+ deficiency may hold promise for treating Leigh syndrome.

Keywords

Leigh syndrome, Ndufs4, Hypoxia, Nicotinamide adenine dinucleotide, NAD, Nicotinic acid, Niacin, Arteriovenous difference, Arterial-venous difference, A-V difference.

Abbreviations

Arterial-internal jugular venous difference	A-IJV difference
Brain tissue PO_2	P_bO_2
Internal Jugular Vein	IJV
Lactate/pyruvate ratio	L/P ratio
Leigh syndrome	LS
Liquid chromatography–mass spectrometry	LC-MS
NADH:ubiquinone oxidoreductase subunit S4	Ndufs4

Oxidized nicotinamide adenine dinucleotide	NAD^+
Reduced nicotinamide adenine dinucleotide	NADH
Nicotinic acid	NA
O_2 content in arterial blood	C_aO_2
O_2 content in IJV blood	$C_{ijv}O_2$
O_2 saturation of hemoglobin in arterial blood	S_aO_2
O_2 saturation of hemoglobin in IJV blood	$S_{ijv}O_2$
Partial pressure of oxygen	PO_2
Partial pressure of oxygen in arterial blood	P_aO_2
Partial pressure of oxygen in IJV blood	$P_{ijv}O_2$
Vehicle	Veh

1. Introduction

Inherited defects of the mitochondrial respiratory chain can produce severe neurological disease in children and adults. Leigh syndrome is the most common pediatric clinical manifestation of mitochondrial disease and is caused by variants in more than 75 different genes [1, 2]. Children with Leigh syndrome appear healthy at birth, but soon thereafter develop progressive neurodegenerative brain lesions, and their median length of survival is 2 years [3]. There is currently no proven therapy to prevent or delay neurodegeneration in patients with Leigh syndrome.

One of the more severe forms of Leigh syndrome is caused by inactivation of the *NDUFS4* gene, which encodes the NADH:ubiquinone oxidoreductase subunit S4 of the mitochondrial complex I [4]. Complex I oxidizes the reduced form of nicotinamide adenine dinucleotide (NADH) to generate NAD^+ and electrons which form the reducing power used to fuel oxidative phosphorylation to produce ATP. Patients with defects in the electron transport chain exhibit an increase in the cytosolic NADH/NAD^+ ratio, which manifests in plasma as an elevated lactate/pyruvate (L/P) ratio.

Mice deficient in *Ndufs4* have decreased activity of mitochondrial complex I and serve as a model of Leigh syndrome by recapitulating many of the neuropathological and clinical features [5]. Although born healthy, *Ndufs4*$^{-/-}$ mice breathing air (21% O_2) die at a median postnatal age of 55 days [5]. Compared to *Ndufs4*$^{-/-}$ mice breathing air, continuously breathing normobaric 11% O_2 prevents and reverses neurological disease and increases lifespan ~5-fold [6, 7]. In

addition to continuously breathing 11% O_2, chronic inhalation of 600 ppm carbon monoxide and chronic anemia also prevent neurological disease and increase survival duration of *Ndufs4*$^{-/-}$ mice [8]. Furthermore, each of these therapeutic strategies is associated with a reduction in elevated brain tissue partial pressure of O_2 (P_bO_2) measured in anesthetized (0.5-1% isoflurane) and mechanically ventilated *Ndufs4*$^{-/-}$ mice using an optical fluorescence PO_2 probe [8]. The most parsimonious explanation for these observations is that brain hyperoxia may be pathogenic in Leigh syndrome.

Sampling blood simultaneously from an artery and a cerebral vein, such as the internal jugular vein (IJV), enables determination of the cerebral arterial-internal jugular venous (A-IJV) difference in blood gas tensions and metabolite levels. Measuring cerebral A-IJV differences of blood gas tensions and plasma metabolite levels has been employed to study the effect of hypoxia on brain metabolism in mammals, such as humans at high-altitude and in simulated-diving Weddell seals [9-12]. However, to our knowledge, this technique has not previously been used in a mouse model of mitochondrial disease.

The objective of this study was to investigate the effect of continuously breathing normobaric 11% O_2 on the brain metabolism of *Ndufs4*-deficient mice by measuring blood gas tensions and the levels of metabolites in simultaneously sampled arterial and cerebral IJV blood. Cerebral A-IJV blood sampling in anesthetized (ketamine 120 mg/kg and fentanyl 9 µg/kg) and mechanically ventilated *Ndufs4*$^{-/-}$ mice breathing air, allowed the detection of reduced cerebral O_2 consumption that produces elevated cerebral venous O_2 levels, which is consistent with the higher P_bO_2 reported previously in these mice [8]. In addition, blood sampling revealed higher brain NADH/NAD^+ ratio, that was accompanied by lower NAD^+ concentrations in the brain. Importantly, breathing 11% O_2 normalized both O_2 and NAD^+ levels in the brain of *Ndufs4*$^{-/-}$ mice. Milder hypoxia (17% O_2) is an ineffective therapy by itself in this model, however we observe a modest improvement in neurodegeneration and survival duration when 17% O_2 is combined with NAD^+ precursor supplementation.

2. Results

2.1 Breathing 11% O_2 for four weeks decreases the elevated PO_2 in internal jugular venous blood of anesthetized and ventilated Ndufs4-deficient mice

To investigate the mechanisms by which chronic hypoxic breathing increases lifespan and improves neurological disease in *Ndufs4*$^{-/-}$ mice, we studied brain oxygenation and metabolism. We measured the partial pressure of O_2 (PO_2) and CO_2 (PCO_2) in simultaneously sampled arterial and IJV blood collected from anesthetized (ketamine 120 mg/kg and fentanyl 9 µg/kg) and ventilated *Ndufs4*$^{-/-}$ and WT mice exposed to either normoxia (breathing air until a postnatal age of ~38 d) or hypoxia (breathing air for the same length of time followed by breathing 11% O_2 for four weeks to a postnatal age of ~66 d).

The partial pressure of O_2 in arterial blood (P_aO_2) supplying the brain was not different between *Ndufs4*$^{-/-}$ and WT mice breathing air (98.8 ± 4.0 vs. 103.0 ± 4.5 mm Hg; *P*=0.57; **Figure 1 A**). In mice breathing air, the partial pressure of O_2 in IJV blood ($P_{ijv}O_2$) leaving the brain, however, was higher in *Ndufs4*$^{-/-}$ mice compared to WT mice (56.0 ± 1.4 vs. 46.5 ± 3.0 mm Hg; *P*=0.006; **Figure 1 B**). The difference between the P_aO_2 in arterial blood supplying the brain and the $P_{ijv}O_2$ in IJV blood leaving the brain is a proxy for cerebral O_2 consumption if cerebral blood flow (CBF) is constant. In mice breathing air, the arterial-IJV PO_2 difference ($P_{a-ijv}O_2$) was smaller in *Ndufs4*$^{-/-}$ mice as compared to WT mice (42.8 ± 16.1 vs. 56.7 ± 19.0 mm Hg; *P*=0.03; **Figure 1 C**). These data suggest that *Ndufs4*$^{-/-}$ mice breathing air have an elevated PO_2 in cerebral IJV blood, which is likely due to impaired O_2 utilization by the brain assuming blood flow is constant.

To quantify O_2 consumption by the brain, we calculated the O_2 content in arterial blood (C_aO_2), the O_2 content in IJV blood ($C_{ijv}O_2$), and arterial-IJV O_2 content difference ($C_{a-ijv}O_2$). O_2 content of blood is determined by PO_2, the O_2 saturation of hemoglobin (SO_2) and hemoglobin concentration. The SO_2 paralleled the PO_2 trends measured in arterial and IJV blood (**Figure S1 A-C**). The concentration of hemoglobin in both arterial and IJV blood was similar between *Ndufs4*$^{-/-}$ and WT mice breathing air (**Figure S1 D & E**). As a result, calculated C_aO_2 was similar between *Ndufs4*$^{-/-}$ and WT mice breathing air (17.5 ± 0.3 vs. 16.6 ± 0.5 ml/dl; **Figure 1 D**). The $C_{ijv}O_2$ trended higher in *Ndufs4*$^{-/-}$ mice compared to WT mice (12.7 ± 0.6 vs. 11.1 ± 0.9; *P*=0.11; **Figure 1 E**). Therefore, the $C_{a-ijv}O_2$ was smaller in *Ndufs4*$^{-/-}$ mice compared to WT mice breathing air (3.9 ± 0.3 vs. 6.4 ± 0.9 ml/dl; *P*=0.01; **Figure 1 F**). These data indicate reduced O_2 consumption in the brain of *Ndufs4*$^{-/-}$ mice breathing air. Interestingly, compared to WT mice, impaired O_2 utilization in the brain of *Ndufs4*$^{-/-}$ mice is visibly evident as the IJV appeared a lighter shade of red, indicating a higher venous SO_2, thus PO_2 (**Figure S2**).

If cerebral O_2 consumption is reduced in *Ndufs4*$^{-/-}$ mice than in WT mice breathing air, a decrease in cerebral CO_2 production would also be expected in *Ndufs4*$^{-/-}$ mice. The total CO_2 carrying capacity of blood (CO_2 content), comprised of the partial pressure of CO_2 (PCO_2) and bicarbonate concentration, was measured in the identical blood samples used to calculate O_2 content; the results mirrored the trends of O_2 content (**Figure S3 A-H**). Thus, in *Ndufs4*$^{-/-}$ mice breathing air, the smaller $C_{a\text{-}ijv}O_2$ correlated with a smaller IJV-arterial CO_2 content difference ($C_{ijv\text{-}a}CO_2$) compared to WT mice breathing air (**Figure 1 G**). These results support the concept of impaired O_2 utilization in the brain of *Ndufs4*$^{-/-}$ mice breathing air.

Since the $P_{ijv}O_2$ likely reflects global brain tissue PO_2 (P_bO_2), a higher $P_{ijv}O_2$ level in *Ndufs4*$^{-/-}$ mice breathing air compared to WT mice may reflect an elevated P_bO_2 [13]. We previously reported that vestibular nucleus P_bO_2 measured with an optical fluorescence O_2 sensor was higher in anesthetized (0.5-1% isoflurane) and ventilated *Ndufs4*$^{-/-}$ mice breathing air compared to WT mice [8]. Therefore, the increased $P_{ijv}O_2$ in *Ndufs4*$^{-/-}$ mice measured by cerebral A-IJV blood sampling in the present study was associated with the elevated vestibular nucleus P_bO_2 levels previously reported (**Figure 1 H**).

In mice breathing 11% O_2, the P_aO_2 was similar between *Ndufs4*$^{-/-}$ and WT mice (45.7 ± 0.9 vs. 45.2 ± 1.2 mm Hg; **Figure 1 A**) but was reduced compared to *Ndufs4*$^{-/-}$ and WT mice breathing air. The $P_{ijv}O_2$ was also similar between *Ndufs4*$^{-/-}$ and WT mice breathing 11% O_2 (34.5 ± 1.0 vs. 35.3 ± 0.6 mm Hg; **Figure 1 B**), and was lower compared to *Ndufs4*$^{-/-}$ and WT mice breathing air. The $P_{a\text{-}ijv}O_2$ did not differ between *Ndufs4*$^{-/-}$ and WT mice breathing 11% O_2 (6.2 ± 2.3 vs. 9.9 ± 2.6 mm Hg; **Figure 1 C**) and reduced compared to *Ndufs4*$^{-/-}$ and WT mice breathing air. The results indicate when *Ndufs4*$^{-/-}$ and WT mice breathe 11% O_2 for four weeks the PO_2 of arterial and IJV blood is reduced to a comparable level in both genotypes.

In *Ndufs4*$^{-/-}$ and WT mice breathing 11% O_2, the concentration of hemoglobin in both arterial and IJV blood was greater than in *Ndufs4*$^{-/-}$ and WT mice breathing air, but did not differ between the genotypes (**Figure S1 F&G**). Despite a compensatory increase in hemoglobin concentration, the C_aO_2 was lower in *Ndufs4*$^{-/-}$ and WT mice breathing 11% O_2 (13.4 ± 0.4 vs. 14.2 ± 0.4 ml/dl; **Figure 1 D**) as compared to *Ndufs4*$^{-/-}$ and WT mice breathing air. The $C_{ijv}O_2$ in *Ndufs4*$^{-/-}$ and WT mice breathing 11% O_2, was similar between *Ndufs4*$^{-/-}$ and WT mice and did not differ from mice breathing air (**Figure 1 E**). Thus, the $C_{a\text{-}ijv}O_2$ decreased similarly in *Ndufs4*$^{-/-}$ and WT mice breathing 11% O_2 as compared to *Ndufs4*$^{-/-}$ and WT mice breathing air (**Figure 1 F**). The results indicate that arterial O_2 content, and likely cerebral O_2 delivery, is reduced when

Ndufs4$^{-/-}$ and WT mice breathe 11% O_2 for four weeks, and this would be expected to lower the PO_2 in IJV blood and brain tissue.

Blood gas tensions and metabolite levels in arterial and IJV blood are influenced by CBF, and CBF is affected by the depth of anesthesia. In our study, anesthesia depth may have differed between the *Ndufs4*$^{-/-}$ and WT mice because *Ndufs4*$^{-/-}$ mice are known to have a slight insensitivity to ketamine [14]. Although we were not able to quantify CBF in *Ndufs4*$^{-/-}$ mice, we instead measured systemic hemodynamics, including heart rate and mean arterial blood pressure, in *Ndufs4*$^{-/-}$ and WT mice undergoing blood sampling. There was no difference in basal heart rate or mean arterial blood pressure between *Ndufs4*$^{-/-}$ and WT mice breathing either air or 11% O_2 (**Table S1**). The results suggest that differences in arterial and IJV blood gas tensions or metabolite levels from *Ndufs4*$^{-/-}$ and WT mice breathing either air or 11% O_2 would not have been driven by changes in systemic hemodynamics.

2.2 Breathing 11% O_2 for four weeks normalizes brain NAD^+ metabolism in Ndufs4-deficient mice

To more broadly explore the metabolic differences between arterial and cerebral venous blood, we performed metabolic profiling of paired arterial and IJV plasma samples collected from anesthetized (ketamine 120 mg/kg and fentanyl 9 µg/kg) and ventilated *Ndufs4*$^{-/-}$ and WT mice exposed to normoxia or hypoxia (described above). Mitochondrial disorders exhibit an elevated L/P ratio in the circulation, which reflects an elevated cytosolic NADH/NAD^+ ratio [15]. Previous reports have shown that circulating lactate is elevated in *Ndufs4*$^{-/-}$ mice breathing air [6, 7, 16], in addition we have previously shown that circulating lactate is normalized by continuously breathing normobaric 11% O_2 [6, 7]. Using liquid chromatography–mass spectrometry (LC-MS), we measured levels of lactate and pyruvate, and calculated the L/P ratio, in paired arterial and IJV plasma samples. We observed a positive linear relationship in L/P ratios between arterial and IJV plasma (**Figure 2 A & B**). Compared to WT mice breathing air, in *Ndufs4*$^{-/-}$ mice breathing air the L/P ratios in IJV plasma were higher for a given L/P ratio in arterial plasma (**Figure 2 A**). In contrast, the correlation of L/P ratios between arterial and IJV plasma were similar between *Ndufs4*$^{-/-}$ and WT mice breathing 11% O_2 for four weeks (**Figure 2 B**). These results likely reflect an increased cytosolic NADH/NAD^+ ratio in the brain of *Ndufs4*$^{-/-}$ mice breathing air, and that breathing 4-weeks of 11% O_2 preserves the NADH/NAD^+ ratio.

Using LC-MS we measured the levels of 126 metabolites (including lactate and pyruvate) in arterial and IJV plasma. To determine the metabolites that are altered by the brain we calculated the arterial-IJV (A-IJV) metabolite level difference for all 126 metabolites (**Table S2**). The A-IJV metabolite level difference was compared by Condition (Hypoxia vs. Normoxia), Genotype (*Ndufs4*$^{-/-}$ mice vs. WT mice), and an Interaction term (Genotype:Condition; **Table S3-5**). We found that the A-IJV difference of nicotinate (vitamin B_3/niacin), a precursor for the biosynthesis of NAD^+, increased in both *Ndufs4*$^{-/-}$ and WT mice breathing air compared to *Ndufs4*$^{-/-}$ and WT mice breathing 11% O_2 (**Figure 2 C**). This difference was driven by a decrease in the nicotinate level in IJV plasma as compared to *Ndufs4*$^{-/-}$ and WT mice breathing air (**Figure S4 A-C**). These data suggest that nicotinate is released from the brain into the venous circulation, and that the amount that is released decreases when mice of either genotype breathe 11% O_2 for four weeks.

Since nicotinate is a metabolic precursor for NAD^+, and neurodegenerative lesions in *Ndufs4*$^{-/-}$ mice are predominatly localised to the brainstem and cerebellum, we sought to determine whether NAD^+ levels are altered in a region specific way. Notably, Lee and colleagues previously reported a decline in whole brain NAD^+ levels in 65 to 75 day old *Ndufs4*$^{-/-}$ mice breathing air [17]. We measured regional brain tissue concentrations of reduced (NADH) and oxidized (NAD^+) NAD forms in ~38 day old *Ndufs4*$^{-/-}$ and WT mice breathing air or after 4-weeks of 11% O_2. In *Ndufs4*$^{-/-}$ mice breathing air, the brainstem concentration of NAD^+ was less than in WT mice (1.31 ± 0.43 vs. 2.36 ± 0.55 nmol/mg protein; *P*=0.01; **Figure 2 D**), but in mice breathing 11% O_2 brainstem NAD^+ concentrations did not differ between *Ndufs4*$^{-/-}$ and WT mice. Similarly, in the cerebellum of mice breathing air, the concentration of NAD^+ trended lower in *Ndufs4*$^{-/-}$ mice as compared to WT mice (5.28 ± 1.10 vs. 7.56 ± 2.64 nmol/mg protein; *P*=0.050; **Figure 2 E**), and were similar between *Ndufs4*$^{-/-}$ and WT mice breathing 11% O_2. In the cerebrum, the concentration of NAD^+ was also decreased in *Ndufs4*$^{-/-}$ mice compared to WT mice breathing air (5.19 ± 0.57 vs. 7.61 ± 2.02 nmol/mg protein; *P*=0.03; **Figure 2 F**), and cerebrum NAD^+ concentrations increased in *Ndufs4*$^{-/-}$ mice breathing 11% O_2 (5.19 ± 0.57 vs. 8.94 ± 2.04 nmol/mg protein; *P*=0.0009) to similar levels found in WT mice (**Figure 2 F**). NADH concentrations in the brainstem and cerebrum did not differ between *Ndufs4*$^{-/-}$ and WT mice breathing either air or 11% O_2 (**Figure S4 D & F**). The NADH concentration in the cerebellum of *Ndufs4*$^{-/-}$ mice breathing air was greater than in WT mice, but similar in mice breathing 11% O_2 (2.89 ± 0.18 vs. 2.47 ± 0.51 nmol/mg protein; *P*=0.03; **Figure S4 E**). The results indicate that in *Ndufs4*$^{-/-}$ mice breathing air the NAD^+ level is decreased in the brainstem, cerebellum and cerebrum, which is preserved by breathing 4-weeks of 11% O_2.

We measured mRNA expression of nicotinate phosphoribosyltransferase (*Naprt*), the rate-limiting enzyme in the biosynthesis of NAD^+ from nicotinic acid (Preiss-Handler pathway [18, 19]) in the brain of *Ndufs4*$^{-/-}$ and WT mice breathing either air or 11% O_2 for four weeks [20]. In *Ndufs4*$^{-/-}$ mice breathing air, the mRNA expression of *Naprt*, was higher in the brainstem (1.38 ± 0.21 vs. 1.00 ± 0.17; *P*=0.008), cerebellum (1.44 ± 0.20 vs. 1.00 ± 0.18; *P*=0.002) and cerebrum (1.58 ± 0.47 vs. 1.00 ± 0.27; *P*=0.007) compared to WT mice breathing air (**Figure 2 G-I**). Moreover, *Naprt* levels did not differ between *Ndufs4*$^{-/-}$ and WT mice breathing 4-weeks of 11% O_2 (**Figure 2 G-I**). The results indicate increased gene expression of the Preiss-Handler pathway, that generates NAD^+ from nicotinic acid, in all brain regions of *Ndufs4*$^{-/-}$ mice breathing air, which is normalised when *Ndufs4*$^{-/-}$ mice breathe 11% O_2 for four weeks.

2. 3 Combining nicotinic acid supplementation with breathing 17% O_2 increases lifespan and delays neurological disease in Ndufs4-deficient mice

Since in *Ndufs4*$^{-/-}$ mice breathing 4 weeks of 11% O_2 normalizes both the $P_{ijv}O_2$ and brain NAD^+ concentrations, and alters brain nicotinic acid metabolism, we hypothesized that pharmacologically replenishing brain NAD^+ levels would prevent neurodegeneration in *Ndufs4*$^{-/-}$ mice. To test this hypothesis, we supplemented *Ndufs4*$^{-/-}$ and WT mice breathing air (21% O_2) with the NAD^+ biosynthetic precursor, nicotinic acid (240 mg/kg twice daily by i.p. *injection*), but observed no benefit to neurological symptoms or lifespan (**Figure S5 E-H**). We next tested nicotinic acid supplementation in the setting of reduced $P_{ijv}O_2$ by treating *Ndufs4*$^{-/-}$ and WT mice breathing 17% O_2. Of note, Ferrari and colleagues have previously shown that chronic exposure to mild hypoxia (17% O_2) alone does not improve either survival duration or the manifestations of neurologic disease in *Ndufs4*$^{-/-}$ mice.

Ndufs4$^{-/-}$ mice that continuously breathe 17% O_2 from 30 days of age will survive for at least three weeks, therefore we measured the $P_{ijv}O_2$ in anesthetized (ketamine 120 mg/kg and fentanyl 9 µg/kg) and ventilated *Ndufs4*$^{-/-}$ mice breathing 17% O_2 for 3-weeks. The $P_{ijv}O_2$ was higher in *Ndufs4*$^{-/-}$ mice breathing air compared to *Ndufs4*$^{-/-}$ mice breathing 3-weeks of 17% O_2 (56.0 ± 4.9 vs. 43.8 ± 2.9 mm Hg; **Figure 3 A**). In *Ndufs4*$^{-/-}$ mice breathing 17% O_2, the $P_{ijv}O_2$ was similar to the $P_{ijv}O_2$ in WT mice breathing air (43.8 ± 2.9 vs. 46.5 ± 9.6 mm Hg; **Figure 3 A**). Thus breathing 17% O_2 for 3-weeks lowers the O_2 tension in IJV blood of *Ndufs4*$^{-/-}$ mice to a comparable PO_2 to WT mice breathing air.

We measured regional brain tissue concentrations of NAD^+ and NADH of *Ndufs4*$^{-/-}$ mice breathing 17% O_2 who were treated with either nicotinic acid or vehicle for three weeks. Brain tissue was harvested 12 h after the previous dose to obtain a trough measurement. In *Ndufs4*$^{-/-}$ mice breathing 17% O_2, nicotinic acid treatment increased trough NAD^+ concentrations in the brainstem (2.06 ± 0.43 vs. 1.26 ± 0.21 nmol/mg protein; *P*=0.02), cerebellum (5.50 ± 0.41 vs. 4.33 ± 0.05 nmol/mg protein; *P*=0.002) and cerebrum (5.77 ± 0.52 vs. 3.96 ± 0.52 nmol/mg protein; *P*=0.003; **Figure 3 B-D**) compared to vehicle treated *Ndufs4*$^{-/-}$ mice breathing 17% O_2. In contrast, NADH concentrations in the brainstem, cerebellum and cerebrum did not differ between nicotinic acid and vehicle treated *Ndufs4*$^{-/-}$ mice breathing 17% O_2 (**Figure S5 B-D**). These data demonstrate that treating *Ndufs4*$^{-/-}$ mice breathing 17% O_2 with nicotinic acid for three weeks modestly increases NAD^+ concentrations in all three brain regions (brainstem, cerebellum and cerebrum).

Survival duration was modestly increased in nicotinic acid-treated *Ndufs4*$^{-/-}$ mice breathing 17% O_2 as compared to vehicle-treated mice (median age of survival of 104 vs. 72 d; *P*=0.003; **Figure 3 E**). Bodyweight was not improved and remained similar between nicotinic acid and vehicle treated *Ndufs4*$^{-/-}$ mice breathing 17% O_2 (**Figure S5 A**). In mice breathing 17% O_2, bilateral neurodegenerative lesions in the vestibular nuclei detected by MRI were observed in 70 day old *Ndufs4*$^{-/-}$ mice treated with vehicle, whereas in older (81-127 day old) *Ndufs4*$^{-/-}$ mice treated with nicotinic acid a single unilateral neurodegenerative lesion in the vestibular nucleus was detected (**Figure 3 F**). From postnatal age 30 to 60 days, in *Ndufs4*$^{-/-}$ mice breathing 17% O_2 and treated with vehicle, both the core body temperature and the latency of the mice to fall off an accelerating rotarod progressively declined, similar to that previously reported in *Ndufs4*$^{-/-}$ mice breathing air (**Figure 3 G & H**)[6, 16, 21]. However, compared to vehicle treated-mice, decrease in core body temperature and the latency to fall from an accelerating rotarod was significantly blunted in nicotinic acid-treated *Ndufs4*$^{-/-}$ mice breathing 17% O_2 at 50 and 60 days of age (**Figure 3 G & H**). The results indicate that the combination of nicotinic acid treatment and breathing 17% O_2 – interventions that individually are not beneficial – modestly increase lifespan and delays neurodegeneration in *Ndufs4*$^{-/-}$ mice.

3. Discussion

We sought to evaluate the effect of continuously breathing normobaric 11% O_2 for four weeks on the brain metabolism of *Ndufs4*$^{-/-}$ mice. As a proxy for brain metabolism, we measured blood gas tensions and the levels of metabolites in arterial and cerebral IJV blood obtained from anesthetized (ketamine 120 mg/kg and fentanyl 9 µg/kg) and mechanically ventilated *Ndufs4*$^{-/-}$ and WT mice breathing either air or after 4-weeks of 11% O_2. Compared to WT mice breathing air, in *Ndufs4*$^{-/-}$ mice breathing air we detected reduced cerebral O_2 consumption (smaller $C_{a-ijv}O_2$) that produced an elevated $P_{ijv}O_2$ and P_bO_2, indicating impaired brain O_2 utilization in *Ndufs4*$^{-/-}$ mice – this result is consistent with our previous report that the brain PO_2 of *Ndufs4*$^{-/-}$ mice is higher [8]. *Ndufs4*$^{-/-}$ mice breathing air had higher L/P ratios in IJV plasma relative to arterial L/P ratios and lower brain tissue NAD^+ concentrations. In both *Ndufs4*$^{-/-}$ and WT mice breathing 4-weeks of 11% O_2, both $P_{ijv}O_2$ and C_aO_2 were reduced indicating chronic hypoxic breathing lowers brain O_2 levels by decreasing O_2 delivery to the brain. In addition, when *Ndufs4*$^{-/-}$ mice breathed 11% O_2 for four weeks, the L/P ratios in IJV plasma and brain tissue NAD^+ concentrations were normalized to WT levels. In both *Ndufs4*$^{-/-}$ and WT mice breathing 4-weeks of 11% O_2, metabolic profiling revealed increased A-IJV difference of the NAD^+ precursor nicotinate, suggesting chronic hypoxic breathing altered nicotinic acid metabolism in the brain. Treating *Ndufs4*$^{-/-}$ mice with a combination of mild hypoxia (17% O_2) and nicotinic acid supplementation, each of which was ineffective, delayed the onset of neurological symptoms and neurodegeneration and increased lifespan, though not as dramatically as breathing 11% O_2.

Impaired peripheral O_2 extraction by skeletal muscle during exercise has been documented in patients with mitochondrial disorders such as mitochondrial encephalopathy, lactic acidosis and stroke-like episodes (MELAS) [22, 23]. Furthermore, decreased brain O_2 consumption has been reported in patients with Leigh syndrome or MELAS measured as a decrease in the cerebral metabolic rate of oxygen ($CMRO_2$) using either PET or MRI [24-27]. We previously reported reduced whole-body O_2 consumption in conscious *Ndufs4*$^{-/-}$ mice breathing air and elevated P_bO_2 measured in the vestibular nucleus of anesthetized (0.5-1% isoflurane) and ventilated *Ndufs4*$^{-/-}$ mice breathing air suggesting impaired brain O_2 utilization [8]. Using cerebral A-IJV blood sampling we now observe decreased cerebral O_2 consumption and reduced cerebral CO_2 production in *Ndufs4*$^{-/-}$ mice breathing air, which is consistent with and may explain the elevated vestibular nucleus P_bO_2. Breathing 11% O_2 for four weeks decreased the $P_{ijv}O_2$ in *Ndufs4*$^{-/-}$ mice due to a reduction in cerebral O_2 delivery, suggested by a lower arterial O_2 content with unchanged systemic hemodynamics.

Metabolite profiling revealed two important results. First, the L/P ratio of IJV plasma is higher for a given arterial L/P ratio in *Ndufs4*$^{-/-}$ mice breathing air, providing metabolic evidence of altered brain metabolism with increased aerobic glycolysis and indicating a higher brain NADH/NAD$^+$ ratio, that is normalized when *Ndufs4*$^{-/-}$ mice breathe 11% O_2 for four weeks. Second, we searched metabolome wide and observed 4-weeks of breathing 11% O_2 consistently increased the A-IJV nicotinate level difference independent of genotype. In follow-up studies we find decreased levels of NAD$^+$ and higher *Naprt* expression in the brainstem, cerebellum and cerebrum of *Ndufs4*$^{-/-}$ mice breathing air, which appeared to be preserved to WT levels *Ndufs4*$^{-/-}$ mice breathed 11% O_2 for four weeks.

We report decreased brainstem and cerebellar concentrations of NAD$^+$ in young (~38 day old) *Ndufs4*$^{-/-}$ mice breathing air. Lee and colleagues have previously reported lower NAD$^+$ concentrations in whole brain tissue collected from older (66-75 day old) *Ndufs4*$^{-/-}$ mice breathing air that would be expected to have severe neurodegenerative lesions [17, 28]. Our findings suggest that NAD$^+$ depletion may precede the development of overt neurodegenerative lesions in the brainstem and cerebellum. Therefore decrement in NAD$^+$ may contribute to neurodegeneration.

NAD$^+$ serves as both an electron carrier and as a substrate for NAD$^+$-consuming enzymes such as sirtuins and poly(ADP-ribose) polymerases (PARPs)[20], the activity of which influence total NAD$^+$ levels in cells and are altered by mitochondrial complex I deficiency [29, 30]. Excessive activation of PARP-1, stimulated by DNA damage, has been reported in *Ndufs4*$^{-/-}$ mice breathing air, and pharmacological inhibition of PARP-1 provides a small but significant delay in the time of onset of neurological symptoms [31]. Although it is unclear exactly how mitochondrial complex I deficiency in *Ndufs4*$^{-/-}$ mice contributes to neurodegeneration, our results show that chronic hypoxic (11% O_2) breathing normalizes P_bO_2 and NAD$^+$ levels.

Other groups have previously tested NAD$^+$ supplementation in *Ndufs4*$^{-/-}$ mice breathing air. For example, while our work was in progress, Lee and colleagues showed that, supplementation of the NAD$^+$ precursor nicotinamide mononucleotide (NMN; 500 mg/kg once every three days i.p injection) in *Ndufs4*$^{-/-}$ mice breathing air improved survival, but not neurological disease [17]. In the current study, we administered to *Ndufs4*$^{-/-}$ mice breathing air a different NAD$^+$ precursor, nicotinic acid, which also failed to improve neurological symptoms, but also did not increase lifespan. The results of these two studies differ slightly possibly because Lee *et al.,* commenced treatment in younger (21 day old) *Ndufs4*$^{-/-}$ mice where pathophysiology would likely be less progressed or due to differences in the pharmacological properties between

the two NAD^+ precursors, however these factors remain to be confirmed. We combined chronic mild hypoxia (17% O_2), an intervention that on its own is not effective in the *Ndufs4*$^{-/-}$ mouse [7], with nicotinic acid *to increase brain NAD$^+$ levels*. This combination provided a small, modest improvement in neurological disease and lifespan. Further investigation using alternative NAD^+ precursors with superior pharmacodynamic and pharmacokinetic properties is warranted.

A limitation of this study is that, for technical reasons, we sampled cerebral venous blood from the extracranial portion of the murine IJV and not intracranially, from the IJV bulb, which may have contaminated cerebral venous blood with venous blood from extra-cerebral sources. A second limitation of our study is that we have not quantified CBF in *Ndufs4*$^{-/-}$ and WT mice, which could in principle impact the observed O_2 and metabolite extractions. This is relevant given *Ndufs4*$^{-/-}$ mice have a slight insensitivity to ketamine [14], however we would have expected the *Ndufs4*$^{-/-}$ and WT mice to be fully anesthetized at the dose (120 mg/kg) ketamine we administered. Moreover, we saw no differences in systemic hemodynamics between genotypes and conditions suggesting anesthetic depth was comparable. In addition, we have previously reported that lower thoracic aortic blood flow, a surrogate measure of cardiac output, did not differ between anesthetized (ketamine 120 mg/kg and fentanyl 9 µg/kg) and mechanically ventilated *Ndufs4*$^{-/-}$ and WT mice breathing air and was unchanged after breathing 11% O_2 for three weeks [32].

In conclusion, we showed that *Ndufs4*$^{-/-}$ mice breathing air have decreased brain O_2 consumption, elevated cerebral venous PO_2 and depleted brain NAD^+ levels, which together may contribute to neurodegeneration. Furthermore, breathing 4-weeks of 11% O_2 normalized cerebral venous PO_2 and brain NAD^+ levels in *Ndufs4*$^{-/-}$ mice. However, at present the precise molecular mechanisms and temporal sequence of events linking mitochondrial defects, O_2, and NAD^+ levels are not known. Our results suggest that hypoxia inspired therapies for mitochondrial disease may benefit from concomitant NAD^+ precursor supplementation.

4. Material and Methods

4.1 Animals

Animal experiments were approved by the Institutional Animal Care and Use Committee of the Massachusetts General Hospital (MGH). *Ndufs4* heterozygous (*Ndufs4*$^{+/-}$) mice on a C57BL6/J background were a kind gift from the Palmiter laboratory, University of Washington. *Ndufs4*$^{+/-}$ mice were bred to generate WT (*Ndufs4*$^{+/+}$) and *Ndufs4*$^{-/-}$ mice. A mix of male and female *Ndufs4*$^{-/-}$ and WT mice were studied. Unless otherwise stated, WT mice breathing air (21% O_2) were a median (interquartile range) postnatal age of 38 d (36-40 d) with a bodyweight of 15 ± 1.7 g (mean ± SD). *Ndufs4*$^{-/-}$ mice breathing air were a postnatal day of 38 d (35-40 d) with a bodyweight of 13 ±1.9 g. *Ndufs4*$^{-/-}$ and WT mice breathing air for ~38 d were placed into hypoxia chambers and continuously breathed 11% O_2 for four weeks. WT mice at the end of breathing 11% O_2 were 70 d (67-79 d) old and weighed 21 ± 3.8 g. *Ndufs4*$^{-/-}$ mice at the end of breathing 11% O_2 were 69 d (68-73 d) old and weighed 16 ± 1.3 g.

4.2 Chronic breathing of air, 17% O_2 or 11% O_2

Mice breathed an inspired O_2 fraction (F_iO_2) of either 21%, 17% or 11%. For A-IJV difference studies, ~38 day old *Ndufs4*$^{-/-}$ mice were used because this age corresponded with peak bodyweight (~15 g) improving successful vessel cannulation [5, 7]. *Ndufs4*$^{-/-}$ mice older than ~38 d breathing air were not studied because from this age *Ndufs4*$^{-/-}$ mice develop progressive neurodegenerative lesions and ultimately die at a median age of ~55 d [5-7, 16, 28]. Breathing 11% O_2 for four weeks was studied because this has previously been shown to prevent, and reverse established, neurodegenerative lesions in *Ndufs4*$^{-/-}$ mice [6, 7].

Mice breathing air were housed in MGH's animal resource facility (Center for Comparative Medicine at MGH). Mice that chronically breathed 11% O_2 were housed in cages kept inside 80 l transparent acrylic boxes used as hypoxia chambers. A F_iO_2 of either 11% or 17% was obtained using a N_2 generator (MAG-20; Higher Peak, Winchester, MA, USA) that concentrated atmospheric N_2 to create a hypoxic gas mixture. O_2 levels were monitored daily using an O_2 sensor (MiniOx 1; Ohio Medical, Gurnee, IL, USA) placed at the outlet port of the hypoxia chamber and was calibrated weekly using an 5.55 % O_2 reference tank (Airgas; Radnor, PA, USA). CO_2 concentrations inside the chamber were kept below 0.4% (monitored using an Extech CO200 Monitor; Extech Instruments, Nashua, NH, USA) using trays containing the CO_2 scavenger soda lime (Sodasorb; Smiths Medical, Minneapolis, MN, USA). Temperature (24–26°C), humidity (30–70%), light cycle (12 h light:dark). Mice housed inside the chambers

were provided food and water *ab libitum*, and additional food pellets were inserted into hydrated gel (Napa Nectar; ScottPharma, Inc., Marlborough, MA, USA) placed on the bedding.

4.3 Femoral arterial and internal jugular venous blood sampling in mice

In young (~38 d old) *Ndufs4*$^{-/-}$ and WT mice, weighing ~13 g, we catheterized the IJV (~200 µm diameter) rather than the larger external jugular vein (~2 mm diameter) because the IJV provides cerebral venous drainage, limiting the contamination of venous blood from extra-cerebral sources [33]. To collect arterial blood the femoral artery was catheterized, rather than the larger common carotid artery, because C57BL6/J mice have an incomplete Circle of Willis and occlusion of a carotid artery might decrease cerebral perfusion [34]. Two catheters implanted retrograde into either the femoral artery or the internal jugular vein (IJV), were constructed from 4 cm long polyurethane BTPU-010 tubing (250 µm outer-diameter; Instech Laboratories, Inc. Plymouth Meeting, PA, USA) inserted 1 cm into the end of polyethylene PE10 tubing 30 cm in length (610 µm outer-diameter; Intradermic; Becton Dickinson, Franklin Lakes, NJ, USA), silicone adhesive was applied to the joint creating an air-tight seal. The opposite end of the PE10 tubing was connected, using a 27-guage needle, to either a fluid-filled pressure transducer or a 1 ml pre-heparinized syringe used for blood sample collection. Before implantation, the catheters were primed with a 10 USP/ml heparin (NDC 0409-2720-02; Hospira, Inc. Lake Forest, IL, USA) saline solution, to remove any air-bubbles and to maintain patency following implantation.

All mice were fasted for between two to six hours before anesthesia induction. Anesthesia was induced via i.p. injection of ketamine (120 mg/kg) and fentanyl (9 µg/kg) in saline. Once anesthetized, mice were secured supine on a heating plate to maintain core temperature at 37 ± 0.5°C via feedback from a rectal temperature probe connected to a temperature controller (TCAT-2; Physitemp Instruments, Clifton, NJ, USA). The cranium was not in contact with the heating plate to avoid directly heating the murine brain. A tracheostomy was performed followed by tracheal intubation for volume-controlled ventilation (Mini Vent 845; Harvard Apparatus, Holliston, MA) at a respiratory rate of 110 breaths/min, a tidal volume of 10 ml/kg of bodyweight, and a positive end-expiratory pressure (PEEP) of 1 cm H_2O. Next, 2 mg/kg of the paralytic rocuronium (NDC 39822-4200-2; X-Gen Pharmaceuticals Inc. Big Flats, NY, USA) was injected i.p. to induce muscle relaxation. Anesthesia and paralysis were maintained

by administering a bolus of one quarter of the induction dose (ketamine 30 mg/kg; fentanyl 2 µg/kg; rocuronium 0.5 mg/kg) i.p. every 10 min. To prevent arterial desaturation during surgical placement of the catheters, thus premature hypoxemia, a F_iO_2 of 30% was used for mice that had previously been breathing air and a F_iO_2 of 21% (air) used for mice previously been breathing either 11% O_2 or 17% O_2.

The right femoral artery was surgically isolated and catheterized retrograde using a catheter (described above) connected to a fluid-filled pressure transducer, Bridge Amp, Powerlab, and LabChart 7 (ADInstruments, Colorado Springs, CO, USA) was used to measure mean arterial blood pressure and heart rate. The murine right internal jugular vein (~200 µm diameter), found parallel and anterior to the right common carotid artery , was surgically isolated and catheterized distal to the sternocleidomastoid muscle. Once inserted the internal jugular venous catheter was fed retrograde until the tip passed distal to the branching point of the right facial vein.

Before arterial and venous blood sampling commenced, *Ndufs4*$^{-/-}$ and WT mice were transfused, via the arterial catheter, with whole blood to prevent a decrease in blood volume, thus organ perfusion, when blood was sampled. All mice used as blood donors were fasted, sex-matched, *Ndufs4*$^{+/-}$ mice kept under identical conditions as the recipient mouse. *Ndufs4*$^{+/-}$ mice were used as blood donors, rather than WT or *Ndufs4*$^{-/-}$ mice because a supply of *Ndufs4*$^{+/-}$ were more readily available. Immediately before arterial and venous blood sampling, whole-blood was collected, via cardiac puncture, into a heparinized syringe from anesthetized (described above) donor mice spontaneously breathing air. The donor blood was stored on ice until needed, then warmed to 37.0°C using a water bath. Once the artery and vein were catheterized (described above), the mice were transfused with 200 µl of pre-warmed donor mouse blood. 200 µl of blood was transfused because a minimum sampling volume of 200 µl was required for metabolic profiling or measuring blood gas tensions in both arterial and venous blood samples.

After both catheters were implanted and the mice were transfused, the F_iO_2 was reduced to the experimental F_iO_2 of either 21% O_2 (air), 17% O_2 or 11% O_2. After allowing time to equilibrate to the experimental F_iO_2, and when mean arterial blood pressure and heart rate were stable, femoral arterial and internal jugular venous blood were drawn simultaneously into 1 ml pre-heparinized syringes (4041-2; Smiths Medical ASD, Inc. Keene, NH, USA). The dead-volume of the PE10 tubing was discarded to limit blood dilution. Upon collection, arterial and venous blood were transferred either to a blood gas analyzer (ABL800 FLEX analyzer;

Radiometer America Inc., Westlake, OH, USA), to measure blood gas tensions (PO_2 & PCO_2) and the concentration of hemoglobin, or into EDTA coated tubes (07 6011; RAM Scientific, Inc. Nashville, TN, USA) followed by centrifugation (2000 g for 10 min at 4°C) to isolate plasma, used for metabolic profiling, that was snap-frozen in liquid N_2 and stored at -80°C.

4.4 Measuring Oxygen dissociation curve (ODC)

Collected blood (20 µl) was diluted with 3 ml of HEMOX solution (HS-500; TCS Scientific Corporation, New Hope, PA, USA) and 6 µl of an anti-foaming agent (AFA-25; TCS Scientific Corporation, New Hope, PA, USA). HEMOX solution contains N-[Tris(hydroxymethyl)methyl]-2-aminoethanesulfonic acid (TES, 30 mM), sodium chloride (135 mM), and potassium chloride (5 mM) in Milli-Q water (pH 7.4). The O_2 dissociation curve (ODC) of the diluted blood sample was measured using a HEMOX analyzer with the sample maintained at 37°C. The partial pressure of O_2 at which 50% of hemoglobin is oxygenated was determined as P_{50} from the ODC. The O_2 saturation of hemoglobin in arterial and IJV blood was determined using the average Hill slope generated from *Ndufs4*$^{-/-}$ and WT mice breathing either air (21% O_2) or after breathing 4-weeks of 11% O_2 (**Figure S1 F**).

4.5 Calculating the O_2 total carrying capacity of blood (O_2 content)

The O_2 content of arterial and IJV blood (C_aO_2 and $C_{ijv}O_2$) was calculated using the formula: O_2 Content = (1.34 × Hb × SO_2) + (0.0031 × PO_2). C_aO_2 - $C_{ijv}O_2$ difference was calculated to determine A-IJV O_2 difference. The CO_2 content of arterial and internal jugular venous blood (C_aCO_2 and $C_{ijv}CO_2$) was calculated using the formula: CO_2 Content = HCO_3^- + (0.0308 × PCO_2). $C_{ijv}CO_2$ - C_aO_2 was calculated to determine $C_{ijv\text{-}a}CO_2$.

4.6 Metabolic profiling using liquid chromatography–mass spectrometry

Metabolic profiling using liquid chromatography–mass spectrometry (LC-MS) was performed on a total of 62 plasma samples (31 arterial and 31 internal jugular venous). In brief, 15 µl of

plasma sample was mixed with 137 µl of ice-cold acetonitrile containing internal standards ($^{13}C_6$ -glucose, D3-lactate, $^{13}C_3$-pyruvate, D3-α-hydroxybutyrate,$^{13}C_2$ -β-hydroxybutyrate, $^{13}C_3$ -alanine & $^{13}C_3$-serine) for metabolite extraction. Samples were vortexed and incubated on ice for 30 min. After centrifugation for 20 min, at 4°C and 21,000 g, 75 µl of sample was transferred to autosampler glass vial for LC-MS analysis and 10 µl of sample was injected on Waters XBridge amide column (2.1 x 100 mm, 2.5 µm; Part # 186006091, Milford, MA, USA). The pooled Quality Control (QC) sample was prepared by mixing ~equal volume of each sample and injected every 12 samples to evaluate the analytical performance. Samples were injected in a randomized order to avoid any run order effect. The column oven temperature was 27°C and the autosampler was 4°C. Mobile phase A was 5:95/acetonitrile:water, 20 mM ammonium acetate, pH 9 (adjusted with ammonium hydroxide) and mobile phase B was acetonitrile. LC gradient conditions at flow rate of 0.220 ml/min were: 0 min 85%B, 0.5 min 85%B, 9 min 35%B, 11 min 2% B, 12 min 2% B, 13.5 min 85%B, 14.6 min 85%B ,15 min 85%B with 0.420 ml/min to 18 min. Dionex Ultimate 3000 UHPLC system was coupled to Q-Exactive Plus Orbitrap mass spectrometer (ThermoFisher Scientific, Waltham, MA, USA) with HESI probe operating in switch polarity mode. MS parameters were: sheath gas flow 50, aux gas flow 10, sweep gas flow 2, spray voltage 2.50 kV in negative & 3.8kV in positive, Capillary temperature 310°C, S-lens RF level -50 and aux gas heater temperature 370°C. Data acquisition was done using Xcalibur (ThermoFisher Scientific, Waltham, MA, USA) in range of: 70-1000 m/z, resolution 70,000, automatic gain control target 3E6 and maximum injection time of 80 ms. Data analysis was done using the Tracefinder™ 4.1. Metabolite annotation was performed based on accurate mass (± 5 ppm) and matching retention time (±0.5 min) as well as MS/MS fragmentation pattern from the pooled QC sample against in-house retention time and MS/MS library of reference chemical standards. The quality of integration for each chromatographic peak was reviewed. Metabolites reported have CV <30% in pooled quality control samples.

4.7 Brainstem, cerebellum and cerebrum tissue collection

Tissue collection was performed between the hours of 10 AM and 6 PM. Unless otherwise stated, a separate cohort of *Ndufs4*$^{-/-}$ and WT mice were used for brain tissue collection to minimize the effect of long-duration anesthesia and surgery on tissue NAD^+ concentrations. A mix of male and female *Ndufs4*$^{-/-}$ and WT mice breathing air from birth until a postnatal age of ~38 d was compared to an older ~66 d old mix of male and female *Ndufs4*$^{-/-}$ and WT mice,

breathing air for the same length of time followed by breathing 11% O_2 for four weeks. Anesthesia was induced using ketamine and fentanyl (described above), a thoracotomy was performed, and the mouse euthanized by exsanguination. An incision was made in to the left and right atria and a needle inserted into the left ventricle, 20 ml of pre-chilled, ice-cold Dulbecco's phosphate buffered saline (DPBS; 14190-144; Life Technologies Limited, Paisley, UK) was perfused throughout the body. Once the expelled fluid ran clear the brainstem, right and left hemisphere of the cerebellum and cerebrum, were rapidly removed on ice, snap-frozen in liquid N_2 and stored at -80°C.

4.8 NADH and NAD^+ tissue quantification

The total concentration of NAD (NADH + NAD^+) and the NADH concentration were measured in the murine right hemisphere of the cerebrum and cerebellum, and in the entire brainstem, previously collected and stored at -80°C. Tissues were homogenized in extraction buffer then centrifuged (4000 g for 5 min) to collect the supernatant. The total NAD concentration and the NADH concentration were measured in the supernatant using a NADH/NAD^+ quantitation colorimetric kit (K337-100; BioVision, Inc., Milpitas, CA, USA) in accordance with manufacturer's protocol . The NAD^+ concentration was calculated by subtracting the total concentration of NADH from the total NAD concentration.

4.9 Quantitative real-time polymerase chain reaction (qPCR)

qPCR was performed similar to that described previously [35]. Total RNA was extracted using TRIzol reagent (15596018; ThermoFisher Scientific, Waltham, MA, USA) from the murine right hemisphere of the cerebrum and cerebellum, and the entire brainstem, previously collected and stored at -80°C. Brain tissue was homogenized (Power Gen 125; Fisher Scientific, Waltham, MA, USA) in TRIzol. After adding chloroform, the sample was vortexed, incubated at room temperature, then centrifuged at 12,000 g at 4°C for 10 min. The top layer was carefully transferred to a new tube. After adding isopropanol, RNA was collected by centrifugation and washed with 75% ethanol. RNA quality and quantity were measured using NanoDrop Lite (ThermoFisher Scientific, Waltham, MA, USA). To synthesize cDNA, High-Capacity cDNA Reverse Transcriptase Kit (4368813; Applied Biosciences, Foster City, CA, USA) was used

according to the manufacturer's instructions. TaqMan Fast Advance Master Mix (Applied Biosystems, Foster City, CA, USA) was used to perform qPCR. TaqMan assay (ThermoFisher Scientific, Waltham, MA, USA) for *Naprt* (Mm00553802_m1). Amplification and real-time quantification of transcripts was performed using a Mastercycler Realplex (Eppendorf, Hamburg, Germany). All reactions were run in duplicate. Expression data in each sample were normalized by the relative cycle threshold (ΔC_T) method to the expression of *18s* ribosomal RNA amplified with TaqMan probe (Hs99999901_s1; ThermoFisher Scientific, Waltham, MA, USA). Relative mRNA expression data were normalized to the WT mice breathing air control group.

4.10 Nicotinic acid administration in Ndufs4$^{-/-}$ and WT mice breathing either air or 17% O_2

30 day old *Ndufs4$^{-/-}$* and WT mice were housed in chambers kept continuously at either 21% or 17% O_2 (described above) and dosed with either vehicle control (phosphate buffered saline; PBS; 14190144; ThermoFisher Scientific, Waltham, MA, USA) or 240 mg/kg nicotinic acid (N4126; Sigma-Aldrich, St. Louis, MO, USA). 240 mg/kg nicotinic acid was used because it is the molar equivalent of a NAD^+ precursor dose, 500 mg/kg nicotinamide riboside, previously reported to increase tissue NAD^+ levels in mice [36]. A solution of nicotinic acid in PBS was prepared under sterile conditions and corrected to pH 7.4 using NaOH, then passed through a 0.022 µM filter. After sterilizing the injection site with an alcohol swab, mice were dosed via i.p. injection at a volume of 10 µl per gram of bodyweight twice a day (AM/PM). Nicotinic acid was administered twice per day due to its relatively short half-life in rodents [37]. Vehicle control mice were injected with PBS.

4.11 Magnetic resonance imaging (MRI)

Mice were continuously anesthetized with 0.5-1.0% isoflurane in room air and images were generated using a DICOM reader (OsiriX; University of Geneva, Switzerland). MRI scans of the brain were performed as previously described , using respiratory gated T2-weighted RARE (rapid acquisition of refocused echoes) MRI images acquired on a 4.7-T small animal scanner (Pharmascan; Bruker, Billerica, MA, USA) with the following parameters: RARE factor: 10, echo

time: 60 ms, repetition time: 6000 ms, Averages: 8, 192 x 192 x 24 image matrix with a voxel size of 0.130 x 0.130 x 0.7 mm).

4.12 Latency to fall from accelerating rotarod measurements

Latency for mice to stay on an accelerating rotarod (Ugo Basile; Stoelting Co., Wood Dale, IL, USA) was performed as previously described . The parameters of the machine were: an acceleration time of 5 rpm/min, maximum speed of 40 rpm and maximum time of 420 s. 3 sets of measurements were performed on mice while breathing air, with the median time reported.

4.13 Statistics

For all data, except data generated by metabolic profiling, statistical analyses were performed using Prism 7 software (GraphPad Software, La Jolla, CA, USA). All data are expressed as mean ± standard deviation (SD). *P*-values <0.05 were considered statistically significant. For a single comparison an unpaired, two-tailed Students T-test was used. For multiple comparisons statistical significance was determined using two-way ANOVA with Sidak's multiple comparisons test. Log-rank (Mantel-Cox) test was used to compare Kaplan-Meier survival curves. For the sake of clarity all pairwise comparisons may not be indicated on every graph. The level of 126 metabolites measured in arterial and internal jugular venous plasma using LC-MS were submitted to statistical analysis. Missing values were imputed at half the minimum of the dataset. All the data were $\log_{10}$ transformed. After imputation and transformation, the arterial-internal jugular venous difference was found. Using the R package *limma*, an interaction model for the arterial-internal jugular venous difference in metabolite levels was fit using Genotype (*Ndufs4*$^{-/-}$ vs. WT) and Condition (Hypoxia vs. Normoxia) as main effects and the interaction term Genotype:Condition [38, 39]. All *P*-values were then corrected for multiple hypothesis testing using the Benjamini-Hochberg procedure as implemented in *limma*. False Discovery Rate (FDR) of <0.05 was considered statistically significant.

Aknowledgements

This work was supported by a gift from the Marriott Family Foundation (V.K.M.) and funds from the Department of Anesthesia, Critical Care and Pain Medicine at Massachusetts General Hospital (W.M.Z.). Conflicts of Interest: V.K.M. and W.M.Z. are co-inventors on a patent application submitted by Massachusetts General Hospital on the use of hypoxia as a therapy. V.K.M. owns equity stake in Raze Therapeutics and is a paid advisor for Janssen Pharmaceuticals and 5AM Ventures.

Conflict of interest

None.

Supplementary data

Supplementary material 1

Supplementary material 2

References

1. Lake, N.J., A.G. Compton, S. Rahman, and D.R. Thorburn, *Leigh syndrome: One disorder, more than 75 monogenic causes.* Ann Neurol, 2016. **79**(2): p. 190-203.
2. Rahman S, T.D. *Nuclear Gene-Encoded Leigh Syndrome Overview.* 2015 [cited 1993-2020 Jan 27 2020]; Available from: https://www.ncbi.nlm.nih.gov/books/NBK320989/.
3. Sofou, K., I.F. De Coo, P. Isohanni, E. Ostergaard, K. Naess, L. De Meirleir, C. Tzoulis, J. Uusimaa, I.B. De Angst, T. Lonnqvist, H. Pihko, K. Mankinen, L.A. Bindoff, M. Tulinius, and N. Darin, *A multicenter study on Leigh syndrome: disease course and predictors of survival.* Orphanet J Rare Dis, 2014. **9**: p. 52.
4. Lake, N.J., M.J. Bird, P. Isohanni, and A. Paetau, *Leigh syndrome: neuropathology and pathogenesis.* J Neuropathol Exp Neurol, 2015. **74**(6): p. 482-92.
5. Kruse, S.E., W.C. Watt, D.J. Marcinek, R.P. Kapur, K.A. Schenkman, and R.D. Palmiter, *Mice with mitochondrial complex I deficiency develop a fatal encephalomyopathy.* Cell Metab, 2008. **7**(4): p. 312-20.
6. Jain, I.H., L. Zazzeron, R. Goli, K. Alexa, S. Schatzman-Bone, H. Dhillon, O. Goldberger, J. Peng, O. Shalem, N.E. Sanjana, F. Zhang, W. Goessling, W.M. Zapol, and V.K. Mootha, *Hypoxia as a therapy for mitochondrial disease.* Science, 2016. **352**(6281): p. 54-61.

7. Ferrari, M., I.H. Jain, O. Goldberger, E. Rezoagli, R. Thoonen, K.H. Cheng, D.E. Sosnovik, M. Scherrer-Crosbie, V.K. Mootha, and W.M. Zapol, *Hypoxia treatment reverses neurodegenerative disease in a mouse model of Leigh syndrome.* Proc Natl Acad Sci U S A, 2017. **114**(21): p. E4241-E4250.
8. Jain, I.H., L. Zazzeron, O. Goldberger, E. Marutani, G.R. Wojtkiewicz, T. Ast, H. Wang, G. Schleifer, A. Stepanova, K. Brepoels, L. Schoonjans, P. Carmeliet, A. Galkin, F. Ichinose, W.M. Zapol, and V.K. Mootha, *Leigh Syndrome Mouse Model Can Be Rescued by Interventions that Normalize Brain Hyperoxia, but Not HIF Activation.* Cell Metab, 2019. **30**(4): p. 824-832 e3.
9. Smith, K.J., D. MacLeod, C.K. Willie, N.C. Lewis, R.L. Hoiland, K. Ikeda, M.M. Tymko, J. Donnelly, T.A. Day, N. MacLeod, S.J. Lucas, and P.N. Ainslie, *Influence of high altitude on cerebral blood flow and fuel utilization during exercise and recovery.* J Physiol, 2014. **592**(24): p. 5507-27.
10. Murphy, B., W.M. Zapol, and P.W. Hochachka, *Metabolic activities of heart, lung, and brain during diving and recovery in the Weddell seal.* J Appl Physiol Respir Environ Exerc Physiol, 1980. **48**(4): p. 596-605.
11. Overgaard, M., P. Rasmussen, A.M. Bohm, T. Seifert, P. Brassard, M. Zaar, P. Homann, K.A. Evans, H.B. Nielsen, and N.H. Secher, *Hypoxia and exercise provoke both lactate release and lactate oxidation by the human brain.* FASEB J, 2012. **26**(7): p. 3012-20.
12. Milledge, J.S. and S.C. Sorensen, *Cerebral arteriovenous oxygen difference in man native to high altitude.* J Appl Physiol, 1972. **32**(5): p. 687-9.
13. Gupta, A.K., P.J. Hutchinson, P. Al-Rawi, S. Gupta, M. Swart, P.J. Kirkpatrick, D.K. Menon, and A.K. Datta, *Measuring brain tissue oxygenation compared with jugular venous oxygen saturation for monitoring cerebral oxygenation after traumatic brain injury.* Anesth Analg, 1999. **88**(3): p. 549-53.
14. Quintana, A., P.G. Morgan, S.E. Kruse, R.D. Palmiter, and M.M. Sedensky, *Altered anesthetic sensitivity of mice lacking Ndufs4, a subunit of mitochondrial complex I.* PLoS One, 2012. **7**(8): p. e42904.
15. Patgiri, A., O.S. Skinner, Y. Miyazaki, G. Schleifer, E. Marutani, H. Shah, R. Sharma, R.P. Goodman, T.L. To, X. Robert Bao, F. Ichinose, W.M. Zapol, and V.K. Mootha, *An engineered enzyme that targets circulating lactate to alleviate intracellular NADH:NAD(+) imbalance.* Nat Biotechnol, 2020. **38**(3): p. 309-313.
16. Johnson, S.C., M.E. Yanos, E.B. Kayser, A. Quintana, M. Sangesland, A. Castanza, L. Uhde, J. Hui, V.Z. Wall, A. Gagnidze, K. Oh, B.M. Wasko, F.J. Ramos, R.D. Palmiter, P.S. Rabinovitch, P.G. Morgan, M.M. Sedensky, and M. Kaeberlein, *mTOR inhibition alleviates mitochondrial disease in a mouse model of Leigh syndrome.* Science, 2013. **342**(6165): p. 1524-8.
17. Lee, C.F., A. Caudal, L. Abell, G.A. Nagana Gowda, and R. Tian, *Targeting NAD(+) Metabolism as Interventions for Mitochondrial Disease.* Sci Rep, 2019. **9**(1): p. 3073.
18. Preiss, J. and P. Handler, *Biosynthesis of diphosphopyridine nucleotide. II. Enzymatic aspects.* J Biol Chem, 1958. **233**(2): p. 493-500.
19. Preiss, J. and P. Handler, *Biosynthesis of diphosphopyridine nucleotide. I. Identification of intermediates.* J Biol Chem, 1958. **233**(2): p. 488-92.
20. Lautrup, S., D.A. Sinclair, M.P. Mattson, and E.F. Fang, *NAD(+) in Brain Aging and Neurodegenerative Disorders.* Cell Metab, 2019. **30**(4): p. 630-655.
21. Quintana, A., S.E. Kruse, R.P. Kapur, E. Sanz, and R.D. Palmiter, *Complex I deficiency due to loss of Ndufs4 in the brain results in progressive encephalopathy resembling Leigh syndrome.* Proc Natl Acad Sci U S A, 2010. **107**(24): p. 10996-1001.
22. Steele, H.E., R. Horvath, J.J. Lyon, and P.F. Chinnery, *Monitoring clinical progression with mitochondrial disease biomarkers.* Brain, 2017. **140**(10): p. 2530-2540.

23. Taivassalo, T., A. Abbott, P. Wyrick, and R.G. Haller, *Venous oxygen levels during aerobic forearm exercise: An index of impaired oxidative metabolism in mitochondrial myopathy.* Ann Neurol, 2002. **51**(1): p. 38-44.
24. Frackowiak, R.S., S. Herold, R.K. Petty, and J.A. Morgan-Hughes, *The cerebral metabolism of glucose and oxygen measured with positron tomography in patients with mitochondrial diseases.* Brain, 1988. **111 (Pt 5)**: p. 1009-24.
25. Lindroos, M.M., R.J. Borra, R. Parkkola, S.M. Virtanen, V. Lepomaki, M. Bucci, J.R. Virta, J.O. Rinne, P. Nuutila, and K. Majamaa, *Cerebral oxygen and glucose metabolism in patients with mitochondrial m.3243A>G mutation.* Brain, 2009. **132**(Pt 12): p. 3274-84.
26. Nariai, T., K. Ohno, Y. Ohta, K. Hirakawa, K. Ishii, and M. Senda, *Discordance between cerebral oxygen and glucose metabolism, and hemodynamics in a mitochondrial encephalomyopathy, lactic acidosis, and strokelike episode patient.* J Neuroimaging, 2001. **11**(3): p. 325-9.
27. Yu, L., S. Xie, J. Xiao, Z. Wang, and X. Zhang, *Quantitative measurement of cerebral oxygen extraction fraction using MRI in patients with MELAS.* PLoS One, 2013. **8**(11): p. e79859.
28. Quintana, A., S. Zanella, H. Koch, S.E. Kruse, D. Lee, J.M. Ramirez, and R.D. Palmiter, *Fatal breathing dysfunction in a mouse model of Leigh syndrome.* J Clin Invest, 2012. **122**(7): p. 2359-68.
29. Alano, C.C., A. Tran, R. Tao, W. Ying, J.S. Karliner, and R.A. Swanson, *Differences among cell types in NAD(+) compartmentalization: a comparison of neurons, astrocytes, and cardiac myocytes.* J Neurosci Res, 2007. **85**(15): p. 3378-85.
30. Karamanlidis, G., C.F. Lee, L. Garcia-Menendez, S.C. Kolwicz, Jr., W. Suthammarak, G. Gong, M.M. Sedensky, P.G. Morgan, W. Wang, and R. Tian, *Mitochondrial complex I deficiency increases protein acetylation and accelerates heart failure.* Cell Metab, 2013. **18**(2): p. 239-50.
31. Felici, R., L. Cavone, A. Lapucci, D. Guasti, D. Bani, and A. Chiarugi, *PARP inhibition delays progression of mitochondrial encephalopathy in mice.* Neurotherapeutics, 2014. **11**(3): p. 651-64.
32. Schleifer, G., E. Marutani, M. Ferrari, P. Sharma, O. Skinner, O. Goldberger, R.M.H. Grange, K. Peneyra, R. Malhotra, M. Weiser, T. Ichinose, D.B. Bloch, V.K. Mootha, and W.M. Zapol, *Impaired hypoxic pulmonary vasoconstriction in a mouse model of Leigh syndrome.* Am J Physiol Lung Cell Mol Physiol, 2019. **316**(2): p. L391-L399.
33. Mancini, M., A. Greco, E. Tedeschi, G. Palma, M. Ragucci, M.G. Bruzzone, A.R. Coda, E. Torino, A. Scotti, I. Zucca, and M. Salvatore, *Head and Neck Veins of the Mouse. A Magnetic Resonance, Micro Computed Tomography and High Frequency Color Doppler Ultrasound Study.* PLoS One, 2015. **10**(6): p. e0129912.
34. Beckmann, N., *High resolution magnetic resonance angiography non-invasively reveals mouse strain differences in the cerebrovascular anatomy in vivo.* Magn Reson Med, 2000. **44**(2): p. 252-8.
35. Hindle, A.G., K.N. Allen, A.J. Batten, L.A. Huckstadt, J. Turner-Maier, S.A. Schulberg, J. Johnson, E. Karlsson, K. Lindblad-Toh, D.P. Costa, D.B. Bloch, W.M. Zapol, and E.S. Buys, *Low guanylyl cyclase activity in Weddell seals: implications for peripheral vasoconstriction and perfusion of the brain during diving.* Am J Physiol Regul Integr Comp Physiol, 2019. **316**(6): p. R704-R715.
36. Giroud-Gerbetant, J., M. Joffraud, M.P. Giner, A. Cercillieux, S. Bartova, M.V. Makarov, R. Zapata-Perez, J.L. Sanchez-Garcia, R.H. Houtkooper, M.E. Migaud, S. Moco, and C. Canto, *A reduced form of nicotinamide riboside defines a new path for NAD(+) biosynthesis and acts as an orally bioavailable NAD(+) precursor.* Mol Metab, 2019. **30**: p. 192-202.
37. Petrack, B., P. Greengard, and H. Kalinsky, *On the relative efficacy of nicotinamide and nicotinic acid as precursors of nicotinamide adenine dinucleotide.* J Biol Chem, 1966. **241**(10): p. 2367-72.

38. R-Core-Team, *R: a language and environment for statistical computing* 2016, R Foundation for Statistical Computing: Vienna, Austria.
39. Ritchie, D.B. and M.T. Woodside, *Probing the structural dynamics of proteins and nucleic acids with optical tweezers.* Curr Opin Struct Biol, 2015. **34**: p. 43-51.
40. Motulsky, H.J. and R.E. Brown, *Detecting outliers when fitting data with nonlinear regression - a new method based on robust nonlinear regression and the false discovery rate.* BMC Bioinformatics, 2006. **7**: p. 123.

Figure 1. **Partial pressure and blood O_2 content in simultaneously sampled arterial and internal jugular venous blood collected from anesthetized and ventilated *Ndufs4*$^{-/-}$ and WT mice breathing air or after 4-weeks of 11% O_2.** Partial pressure of O_2 was measured in (**A**) arterial (P_aO_2) and (**B**) internal jugular venous ($P_{ijv}O_2$) blood. (**C**) Arterial-internal jugular venous PO_2 difference ($P_{a-ijv}O_2$). Blood O_2 content was measured in (**D**) arterial (C_aO_2) and (**E**) internal jugular venous ($C_{ijv}O_2$) blood. (**F**) Arterial-internal jugular venous O_2 content difference ($C_{a-ijv}O_2$). (**G**) Pearson correlation between the arterial-internal jugular venous O_2 content difference ($C_{a-ijv}O_2$) and the internal jugular venous-arterial CO_2 content difference ($C_{ijv-a}CO_2$) in *Ndufs4*$^{-/-}$ mice (r =0.80, P<0.002) and WT (r =0.97, P<0.0001) mice breathing air. (**H**) $P_{ijv}O_2$ plotted against values previously reported in the vestibular nucleus brain tissue PO_2 (P_bO_2) of *Ndufs4*$^{-/-}$ and WT mice breathing either air or 11% O_2 [8]. Statistical significance was determined using two-way ANOVA with Sidak's multiple comparisons test. Data are mean ± SD.

Figure 2. Lactate/pyruvate ratios and nicotinate levels measured in simultaneously sampled arterial and internal jugular venous plasma, brain tissue concentration of NAD^+ and *Naprt* mRNA expression, collected from *Ndufs4*$^{-/-}$ and WT mice breathing air or after 4-weeks of 11% O_2. Pearson correlation between arterial and internal jugular venous plasma lactate/pyruvate ratios in (**A**) *Ndufs4*$^{-/-}$ (r=0.78, P=0.012) and WT (r=0.77, P=0.016) mice breathing air or in *Ndufs4*$^{-/-}$ (r=0.98, P<0.0001) and WT (r=0.97, P=0.005) mice breathing 4-weeks of 11% O_2. (**C**) Volcano plot of the arterial-internal jugular venous (A-IJV) metabolite level difference depicting on the X-axis log_2fold-changes (log_2FC) and on the Y-axis statistical significance in Condition (Hypoxia vs. Normoxia) as -log_{10} P-values in both *Ndufs4*$^{-/-}$ and WT mice breathing 4-weeks of 11% O_2 (Hypoxia) compared to both *Ndufs4*$^{-/-}$ and WT mice breathing air (Normoxia). Tissue concentration of NAD^+ measured in the (**D**) brainstem, (**E**) cerebellum and (**F**) cerebrum. Tissue mRNA expression of *Naprt* measured in the (**G**) brainstem, (**H**) cerebellum and (**I**) cerebrum. Statistical significance was determined using two-

way ANOVA with Sidak's multiple comparisons test. All *P*-values generated from metabolic profiling were corrected for multiple hypothesis testing using the Benjamini-Hochberg procedure and false-discovery rate (FDR) <0.05 considered statistically significant. For Pearson correlation the ROUT method (Q = 0.5%) was used to identify and exclude 1 outlier [40]. n.s.= non-significant. Data are mean ± SD.

Figure 3. Nicotinic acid treatment provides a modest increase in lifespan and delay in the time of onset of neurological symptoms and neurodegenerative brain lesions of *Ndufs4*$^{-/-}$ mice breathing 17% O_2. (**A**) The partial pressure of internal jugular venous blood ($P_{ijv}O_2$) in *Ndufs4*$^{-/-}$ mice breathing 17% O_2 for 3-weeks compared to the same $P_{ijv}O_2$ values for *Ndufs4*$^{-/-}$ and WT mice breathing air (21% O_2) taken from Figure 1. Tissue concentration of NAD^+ measured in the (**B**) brainstem, (**C**) cerebellum and (**D**) cerebrum of *Ndufs4*$^{-/-}$ mice breathing 17% O_2 for 3-weeks and treated with either vehicle or nicotinic acid (NA; 240 mg/kg twice daily by *intraperitoneal injection*). Brain tissue was harvested 12 h after the previous dose. (**E**) Survival duration, (**F**) MRI images of the vestibular nuclei (arrow used to indicate a lesion), (**G**) latency to fall from an accelerating rotarod and (**H**) core body temperature of *Ndufs4*$^{-/-}$ and WT mice breathing 17% O_2 and treated with either vehicle or NA. For a single comparison an unpaired, two-tailed, Students T-test was used. For multiple comparisons statistical significance was determined using two-way ANOVA with Sidak's multiple comparisons test. Log-rank (Mantel-Cox) test was used to compare Kaplan-Meier survival curves. Data are mean ± SD.